RESIDUAL STRESSES IN HEAT TREATMENT

O.N.Mohanty
TATA STEEL
Jamshedpur

1.0 INTRODUCTION

There are two kinds of stresses that an object may be subjected to:

(a) Applied Stress - which is due to external forces acting on the object.

(b) Residual Stress - which remains in the object after all the applied forces have been removed.

The basic cause of residual stress is non-uniform plastic flow due to previous operations. Some specific causes are heat treatment, welding, mechanical operations such as cold working, grinding & so on. Residual stresses must form a balanced force system within the object, which implies that a residual compressive stresses in one part of an object must be balanced by residual tensile stress in another part.

Residual stresses may be harmful or beneficial. When tensile in nature, it adversely affects the fatigue properties in particular & ductility in general. When it is compressive in nature, as for example, in carburizing or after induction/flame hardening, the fatigue properties improve. Another example of beneficial compressive stress is the steel reinforced pre-stressed concrete.

Residual and applied stresses add algebraically, as long as their sum does not exceed the elastic limit. It is therefore necessary for a designer to know the level and nature of the residual stress so that he could prescribe safe levels of applied stress for an engineering component.

Residual stresses could be introduced into metals and other materials through any of the processes. Examples (Fig.1) show some of these, as given below :

(a) Mechanical : Surface Working, Forming, Assembling,
(b) Chemical : Oxidation, Corrosion, Electroplating.
(c) Thermal : Welding, Casting, Heat Treatment, and
(d) Combinations of above : Cold-Working induced phase transformation.

In the present article, an attempt will be made to cover the Residual Stresses generated through thermal means and with special emphasis on Residual Stresses through Heat Treatment. There are several methods of measuring residual stress. Some of these are:

(a) Mechanical Relaxation,
(b) Acoustic Wave Techniques, and
(c) X-Ray Diffractometry.

Basic principles of these will be dealt with in the paper with some details of the X-Ray Diffractometry.

2.0 THERMAL PROCESSES & RESIDUAL STRESSES

Residual Stresses arising from thermal processes could be classified as those with:

2.1 Thermal gradient alone, and
2.2 Thermal gradient in combination with phase transformation.

These could be dealt with in some details.

2.1 Residual Stresses With Thermal Gradient Alone

Examples of this variety include quenching, casting & welding.

2.1.1 Residual Stresses during Quenching:

If we consider the volume change due to thermal gradient only, at the start of cooling the surface cools faster than the core (interior). The temperature difference between the core and surface increases upto certain time till it reaches a maximum. As a result, after a short time, the surface contracts more than the interior creating a pressure against the core. Since the core does not contract by the same amount, this creates a condition of tension in the rigid outer shell & compression in the core; irreversible plastic flow can then occur. The picture is given in Fig.2a. With time, there is a further lowering of temperature & situation changes. Further decrease of temperature results in longitudinal compressive

stress at surface and tensile stress at the core. Fig.2a is a schematic representation of distribution of residual stresses over the diameter of a quenched bar in longitudinal, tangential and radial directions. The actual value of the peak residual stress in quenching can increase by the (i) Quenching temperature and (ii) Quenching power of the coolant, (iii) Section size, (iv) Modulus of elasticity, and (v) Coefficient of thermal expansion.

2.1.2 Residual Stress During Casting:

As in the case of quenched cylinders, castings which undergo no phase transformation would normally have compressive stresses at the surface & tensile stresses in the interior. The situation however can get complicated through the following:

(a) mechanical restraint that a mould can offer as in permanent moulding or die-casting,
(b) artificial cooling rates (i.e. chills) introduced into the casting, and
(c) section-size of casting.

2.1.3 Residual Stresses in Butt Welding:

Considering a flat plate, butt welded along a line, the longitudinal stress (parallel to the weld line) a stress pattern as given in Fig.1(C) can result. This can be explained as follows: as the weld metal & heat affected zone shrink during cooling, they are restricted by the cool surrounding areas. Longitudinal tensile stresses thus result in the weld zone, balanced by compressive forces in the nearby region.

2.2 Residual Stresses During Thermal Gradient And Phase Transformation (Quench Hardening)

Here, the effects of phase transformation are superimposed on those from thermal gradient, as during Quench Hardening of steels. This can be dealt with in two situations:

2.2.1 Quenching of Direct Hardening Steels, and
2.2.2 Carburizing of Steels.

As an aid in understanding the situation, the specific volumes of various phases associated with transformations in steels are given in Fig.3.

2.2.1 Residual Stress During Quenching of Direct Hardening Steels:

The residual stress pattern developed depends upon various factors. However, every product of austenite decomposition, i.e., martensite, bainite or pearlite would be associated with a volume increase (Fig.3). The situation is schematically depicted in Fig.2(C & C1) for a through-hardened steel. Fig. 2(C2) depicts the picture where the steel is partially hardened. Upon quenching a steel, martensite forms instantly on the surface layer, associated with volume expansion, where as the interior remains as austenite because it is still hot. Afterwards when the interior austenite changes to martensite, the volume expansion due to transformation is restricted by the hardened surface layer resulting in compression in the core and tension at the surface. At the same time thermal contraction in the core is hindered by the hard surface layer. Fig.2(c) also depicts the situation when net-volume expansion is larger than thermal contraction. In some cases this type of volume change may cause plastic deformation leading to distortion of the heat treated part or even localized rupture (Quench Cracking).

Large size of the component and high cooling rate contribute to large thermal contraction as compared to volumetric expansion. For a fixed quenching rate the thermal gradient decreases with decreasing cross section resulting in decrease of residual stress.

Fig.4 shows residual stress patterns along with CCT diagrams of DIN 22 Cr 44 steel of the surface (s) and centre (C) of different diameter. The complexity of the residual stress pattern depends upon (i) component size (ii) quenching rate and (iii) hardenability of steel. The residual stress pattern can be modified with different transformation characteristics or, during tempering and finish machining operations.

2.2.2 Residual Stress During Surface Hardening:

During carburizing and quenching of low carbon steels the core materials transform to ferrite and pearlite with attendant stress relaxation of stresses developed due to any transformation. This occurs around 600 - 700^{0}C. Below 300^{0}C the carburised case transforms to martensite with minimum stress relaxation. Residual compressive stress develops in the case with maximum at the surface. The presence of retained austenite causes the maximum residual stress to develop at a depth below the

surface (Fig.5a). The amount of retained austenite depends on (i) steel composition (ii) carbon content of the case (iii) quenching temperature and (iv) the severity of quenching. The case/core interface region experiences the reversal sign of residual stress. Fig.5b describes the residual stress for a carburised 9340 steel. The position of maximum compressive stress depends upon several factors such as, total case depth, severity of quench, steel hardenability etc.

In nitriding also a compressive residual stress develops in the surface layer. Low temperature nitriding imparts more residual stress as compared to high temperature nitriding.

In nitro carburising residual compressive stresses increases with hardness and depth of diffusion zone and decreases with increasing carbon and alloy content.

In induction hardening the core remains unchanged while the martensite forms on the surface causing a surface residual compressive stress. As in carburizing, the residual compressive stress usually increases upto a certain depth below surface. Fig. 6 shows the situation for induction hardened and tempered 1045 steel. Transition to tensile stress takes place near the hardness drop off between case and unhardened surrounding material and then fades away to zero stress with the increase in distance.

2.3 Control Of Residual Stresses:

Table I gives typical values of maximum residual stresses in the surface hardened steels, showing clearly the influence of tempering on residual stress level. Tempering at around 150^0C retains 50 - 60% of the residual stresses developed during quenching. Higher tempering temperatures greatly reduces the surface compressive stress. Stress relief temperature around 600^0C is used for mechanically deformed parts or, parts with tensile residual surface stresses. Dangerous level of residual tensile surface stresses may also be removed by gentle grinding on the surface.

3.0 Methods Of Stress Measurement

3.1 General Methods

In the Hole-Drilling technique, care has to be taken to ensure avoiding introduction of other stresses (there are also micro hole drilling techniques at the research level which are more or less non-destructive). The basic principle of the test lies in the fact that when a hole is drilled on to a stressed body, there is stress relaxation that can be computed from strain gauges fixed on to the surface (for measuring the strain in the immediate vicinity of the hole). The method in general is described as, `semi-destructive' since the small hole (1.5 - 3mm in dia & depth) drilled does not impair the integrity of the component in many cases. The drilled hole can also be plugged subsequently.

In the Acoustic Wave propagation method, one depends on the fact that:

$\sigma = M.\varepsilon + C.\varepsilon^2 +$

$\therefore \sigma \approx (M+C\varepsilon).\varepsilon \approx M'\varepsilon$, where M, C are constant similar to modulii. Again,

$V = K\sqrt{(M+C\varepsilon)}$

where, V = sound velocity; ε = state of strain; M = elastic constant and K = material constant

Thus, one can determine strain values (ε) and using that, the stress (σ).

The Electro Magnetic Techniques (EMT) are broadly based on three methods: Barkhausen noise, Non-linear harmonics and Magnetically Induced Velocity Changes (MIVC). The principles of only one of them, namely, the Barkhausen noise is shown in Figures 7 to 9. The magnetic Barkhausen method is dependent on the stress as well as relative direction of the applied magnetic field of the stress direction (Fig.10). The figures show a typical stress dependence of the inductively detected Barkhausen noise in a ferrous material. In this case, where the magnetic field and the stress are parallel, the Barkhausen amplitude increases with tension and decreases with compression. However, in the case where these two are perpendicular, the opposite result is obtained. The behaviour shown in Fig.10 holds good for material with a positive magneto striction co-efficient. The inductively detected Barkhausen method reveals stress effects occurring near the surface (about 0.1mm). The effective stress measuring range is upto about 50 per cent of the yield stress of the material; the Barkhausen noise gets saturated at very high stress levels.

Apart from using magnetic effect of Barkhausen noise for stress determination, some research has also been done on the acoustic effect of Barkhausen noise in which the magnetic field is applied parallel to the stress direction. However, such data do not show a distinct trend for compression and tension regions - the signal can show a maximum (Fig.11). The acoustic Barkhausen noise therefore cannot distinguish tension from compression. Research is still on, in this area.

The magnetic Barkhausen measurement can be done within a few seconds. Continuous measurement at a slow scanning speed (10mm/second) is also possible. Preparation of surface is generally not required. The method can be made field-useable. However, one should keep in mind that the signals of Barkhausen tests are also sensitive to factors not related to stress, such as microstructure, heat treatment or material variation. It is therefore necessary that a careful calibration of the data is done to improve the reliability. Examples of inductive Barkhausen noise technique include measurement of residual welding stress, grinding damages in bearings and residual hoop stress in railroad wheels.

3.2 Residual Stress Measurement By X-Ray Diffractometry:

Some of the salient features of the measurement of the residual stress using XRD are:

* basically non-destructive.
* only surface stress (degree of penetration is about 10-15 u) can be measured. However, by etching out layers, it is possible to examine interior surfaces; but in this case, the method becomes destructive (and allowances for removal of upper surfaces to be made).
* no stress free samples are ordinarily required. Stress measurement can be done representing macro-level (surface) or micro-level in individual phases.

The basic principle of (surface) macro-residual stress lies in the fact that there is a shift in the peak of an X-ray line, proportional to the amount of stress; thus interplanar distance acts as the transducer. On the other hand, the micro residual stress is primarily dependent on broadening (increase in mid-width) of an X-ray line. One can examine the principle by starting with:

Bragg equation $2d \sin\theta = n\lambda$

where, d = interplanar distance; θ = Bragg angle; λ = wave length of X-ray radiation

Differentiating the equation, $\Delta d/d = -\cot\theta/\Delta\theta$

Therefore, for the same strain ($\Delta d/d$), shift ($\Delta\theta$) will be high (accuracy high for high angles, cot θ low). Thus one uses a high angle line. Typically for steel, one could use Cr K_α radiation & 211α plane that occurs around 152 degrees (2θ). Broadly, for the accurate stress measurement, one requires:

* correct values of X-ray elastic constant (XEC) specific to the appropriate plane (in the above example, 211 plane)
* accurate line position determination.

The XEC are determined for the specific planes by applying known stresses on to samples. Further, the apparent peak position does not match with the actual peak position. There are several methods for determining the actual peak position.

One of the most popular is passing a parabola through points which are within 85 per cent of the apparent peak intensity; prior to this, the necessary corrections (absorption, polarization, etc.) are made on the intensity of points. There are also methods which use the centroid of a line profile as the indicator of the peak position.

The operating equation for stress (σ) measurement is given as:

$$\sigma_\phi = (2\theta_\perp - 2\theta_\psi)\ \mathrm{Cot}\frac{\theta}{2}\ \frac{E}{1+\nu}\ \frac{1}{\mathrm{Sin}^2\psi}\ \frac{\pi}{180}$$

where, E, ν = Young's modulus & Poission's ratio respectively for the chosen crystallographic plane

$\theta_\perp$ = Bragg angle at $\psi = 0$ position (ψ is the angle between sample perpendicular & plane perpendicular); Ψ = Angle of rotation from $\psi = 0$ position

The slope of the plot between $\Delta 2\theta$ & $\mathrm{Sin}^2\psi$ yields the strain

The main developments in the technique over the last decade encompass the following:

Use of smaller tubes and position sensitive detectors for field use. On the software side, the developments include taking measurements on both

positive and negative rotation and computing the shear stress from the data.

The advantage with position sensitive detector lies in the fact that one can scan the entire line profile in a matter of seconds and accumulate sufficient counts for high accuracy. There are mobile/portable units now available for making use of all the features mentioned above. A high multiplicity line [732 + 651] is also used with MoK_{α} in textured steels for averaging out the effect of texture & yielding a better linearity between $\Delta 2\theta$ & $Sin^2\psi$.

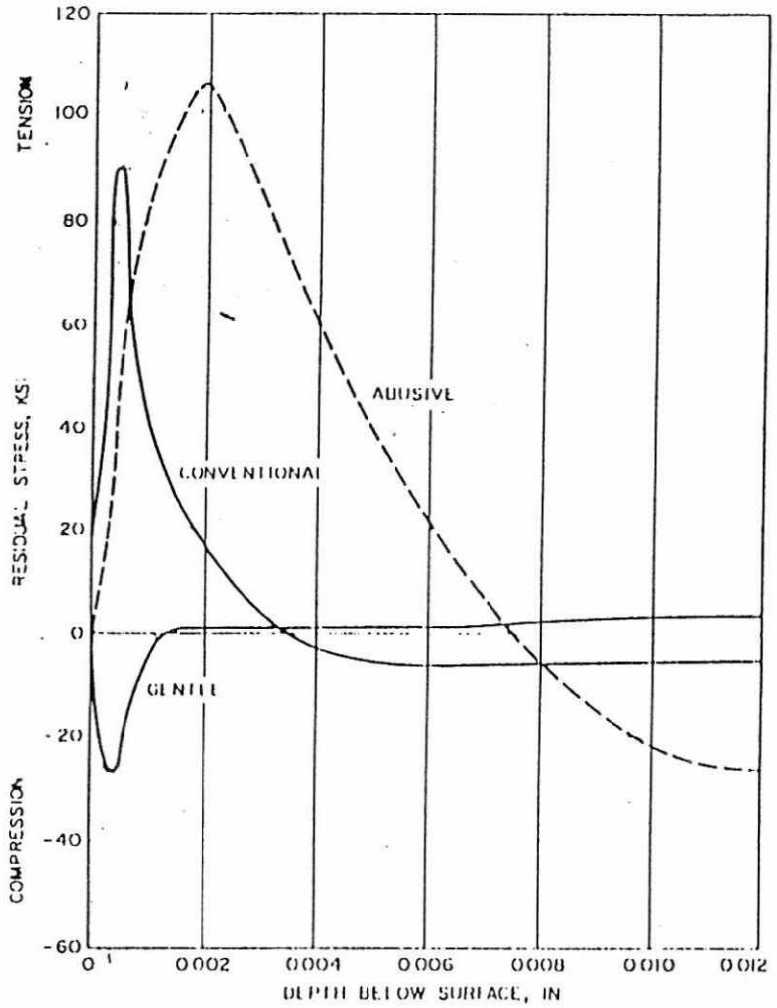

	GRINDING CONDITIONS		
	GENTLE	CONVENTIONAL	ABUSIVE
WHEEL	A46HV	A46KV	A46MV
WHEEL SPEED, FT/MIN	2000	6000	6000
DOWN FEED, IN/PASS	"LS"	0.001	0.002
GRINDING FLUID	SULF OIL	SOL OIL (1:20)	DRY

Fig. 10. Typical residual stress distributions after gentle and normal grinding of hardened steel (stress measured in direction of grinding)

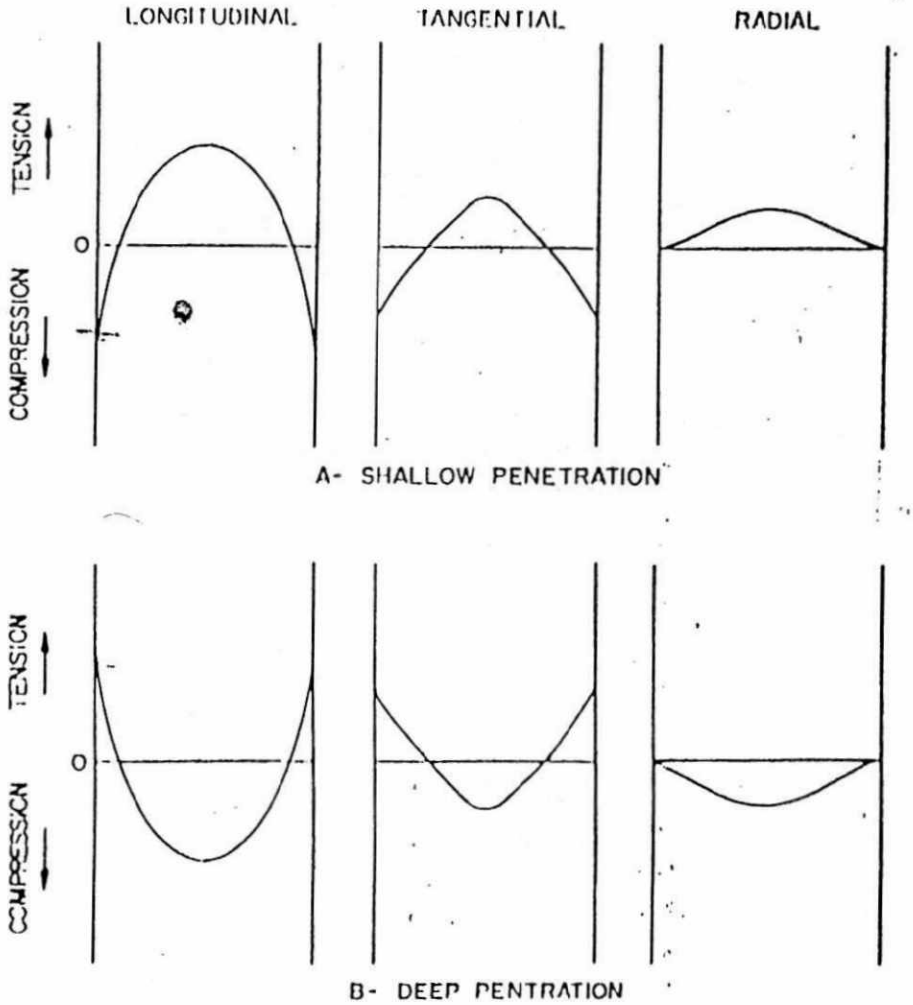

Fig. 16 b- Idealized residual stress patterns found in shallow-drawn rods (no phase transformation)

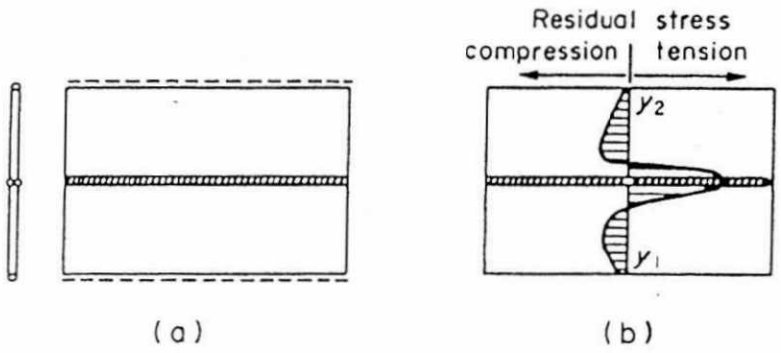

Fig. 16. The transverse shrinkage occurring in (butt) weldments. (b) Longitudinal residual stress patterns in the weldment and surrounding regions.

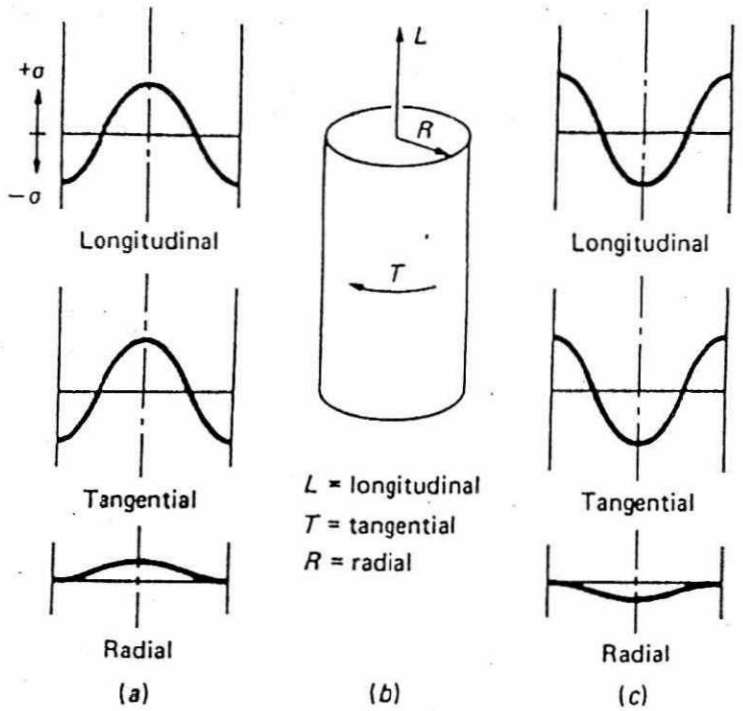

Fig. 2 Schematic illustration of the distribution of residual stress over the diameter of a quenched bar in the longitudinal, tangential, and radial directions due to (a) thermal contraction and (c) both thermal and transformational volume changes. (b) Schematic illustration of orientation of directions.

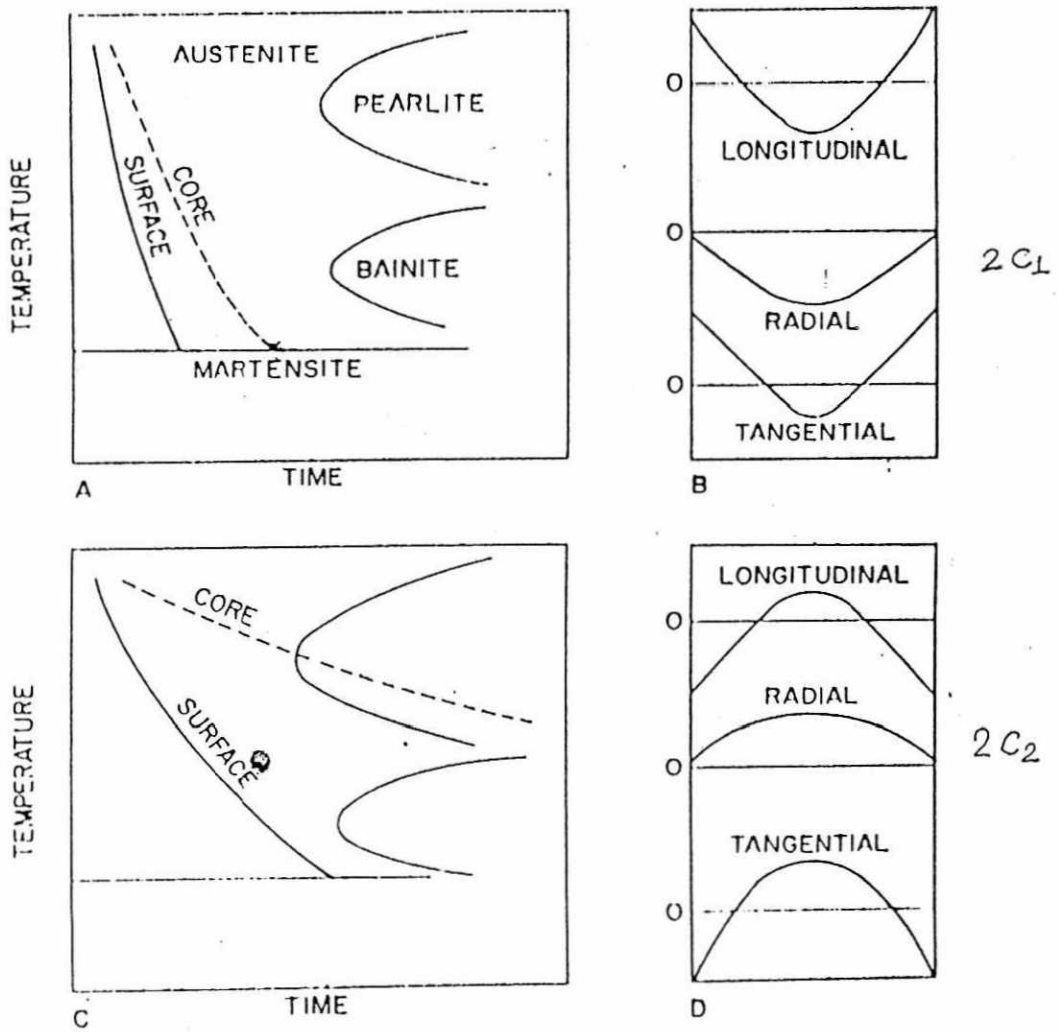

Fig. 2C1 & 2C2 Residual stress patterns developed on quench-hardening a steel cylinder. Cooling curves for the surface and core regions of the part are shown relative to the TTT diagram

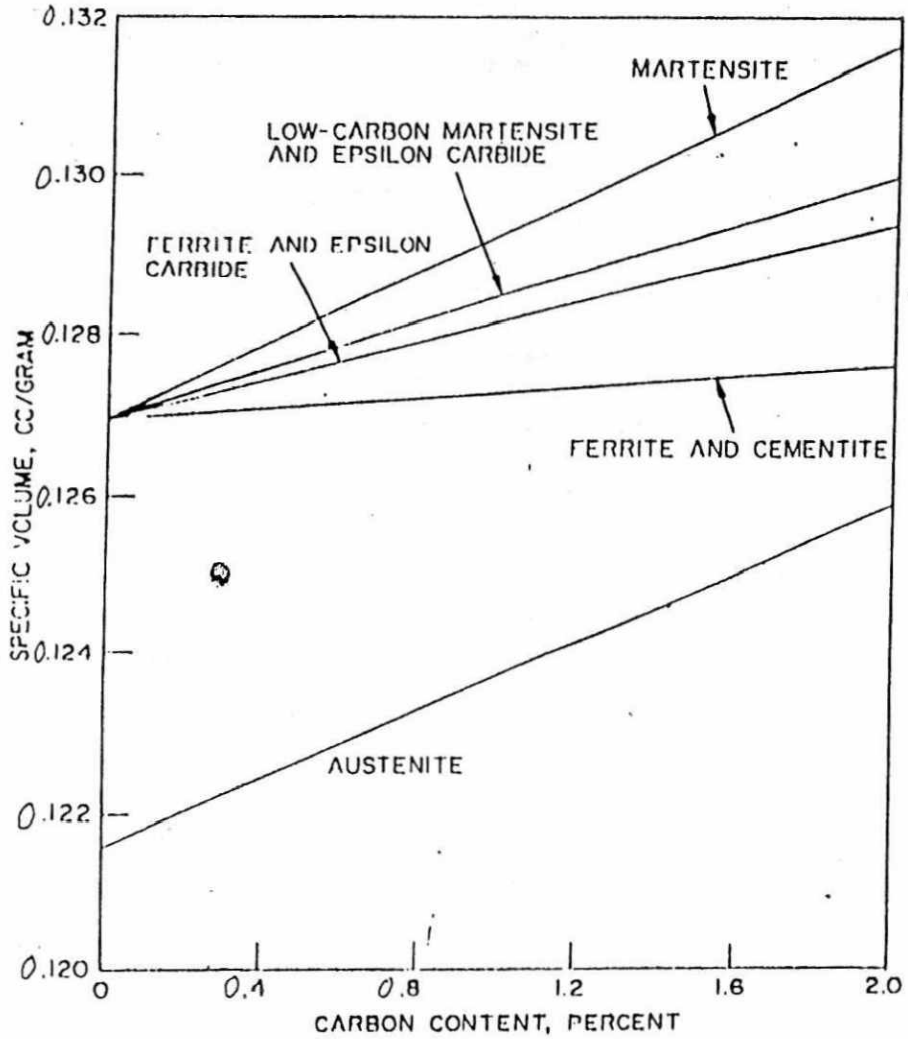

Fig. 3 - Specific volumes of steel phases versus carbon content

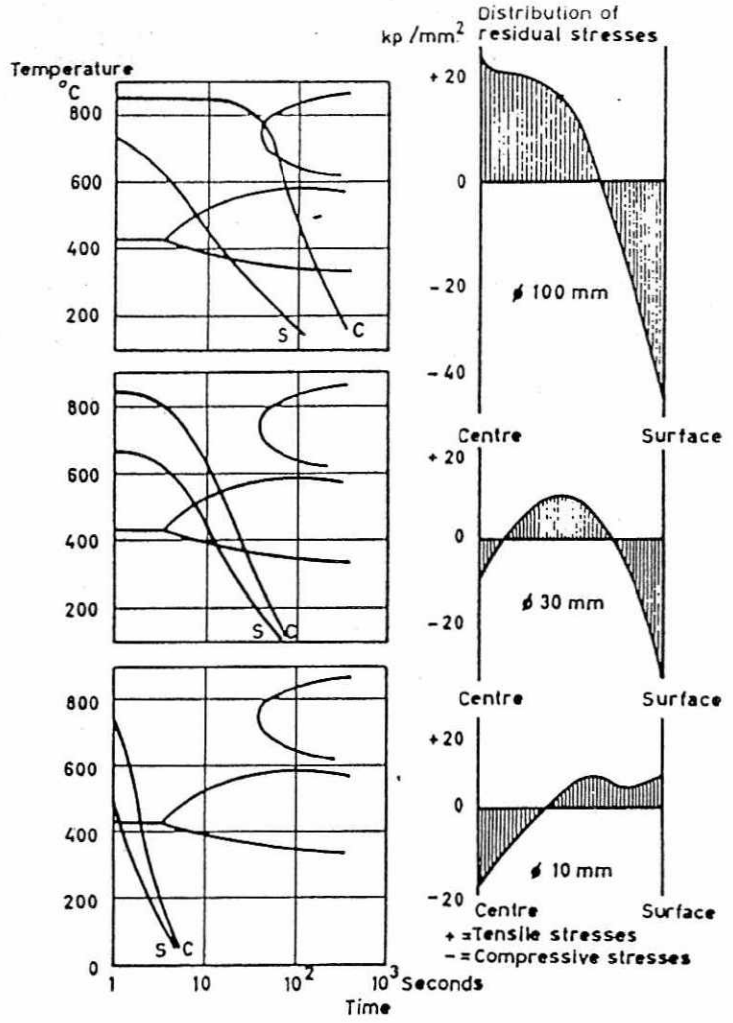

Fig. 4 (Left) Continuous cooling transformation diagrams of DIN 22 Cr Mo 44 steel showing austenitic decomposition with the superimposed cooling curves of the surface (s) and center (c) during water-quenching of round bars of varying dimensions. (Right) The corresponding residual stress pattern developed due to thermal and transformational volume changes.

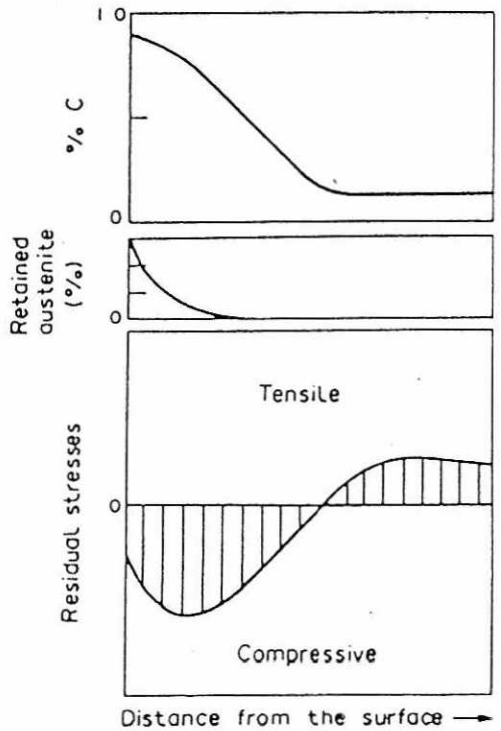

Fig. 5a Relationship between carbon content, retained austenite, and residual stress

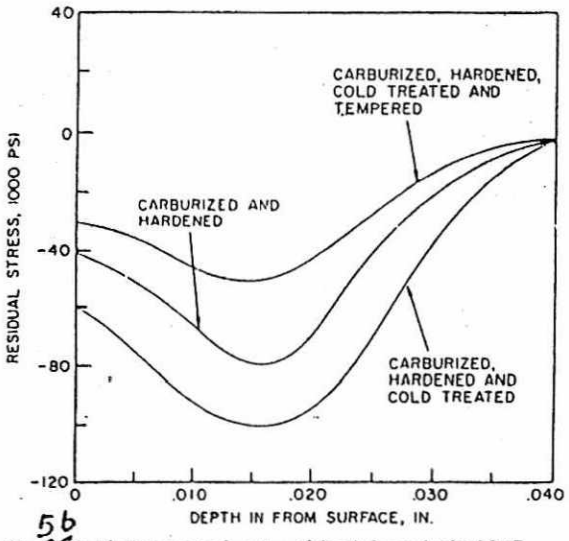

Fig. 5b Residual stress as a function of depth for carburized SAE 9310 steel (Ref. 9)

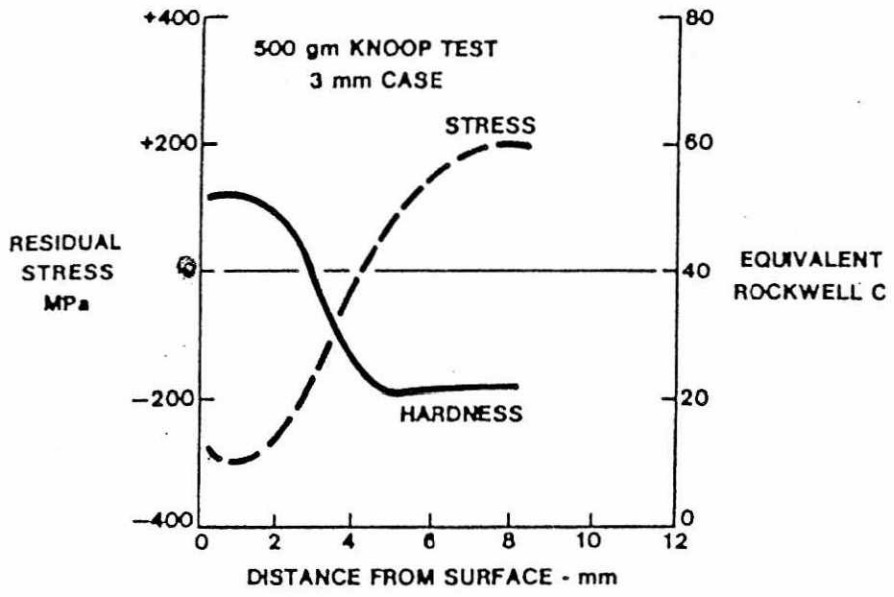

Fig. 6 A typical hardness and residual stress profile in induction-hardened (to 3-mm case depth) and tempered (at 260°C) 1045 steel.

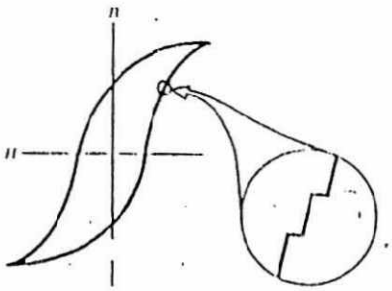

Fig. 7 Hysteresis loop for magnetic material showing discontinuities that produce Barkhausen noise. Source: Ref 2

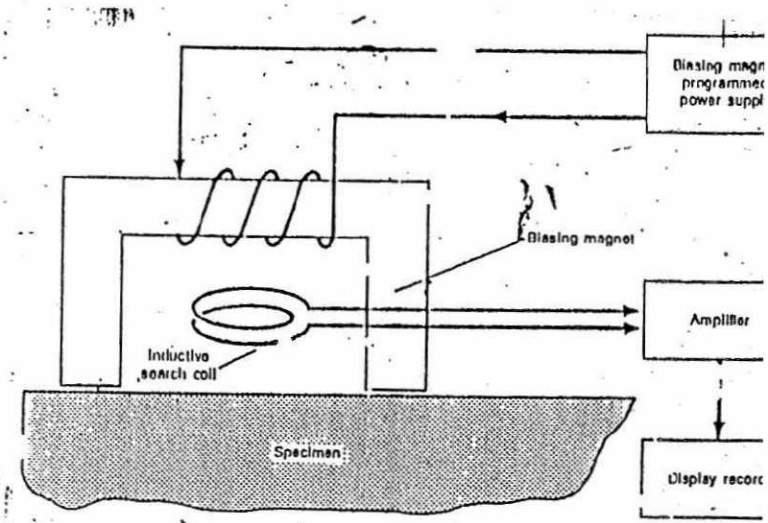

Fig. 8 Arrangement for sensing the Barkhausen effect

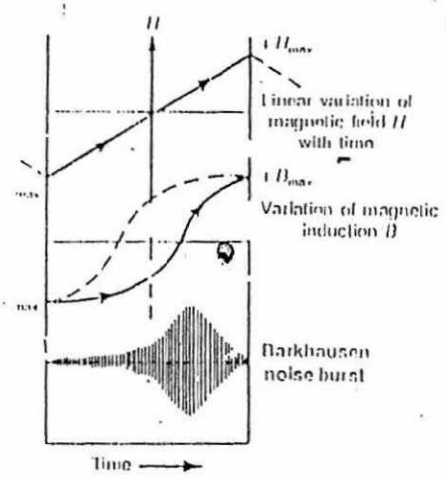

Fig. 9 Schematic showing the change in magnetic field H with time, variation in flux density during the same period, and the generation of the Barkhausen noise burst as flux density changes. Source: Ref 14

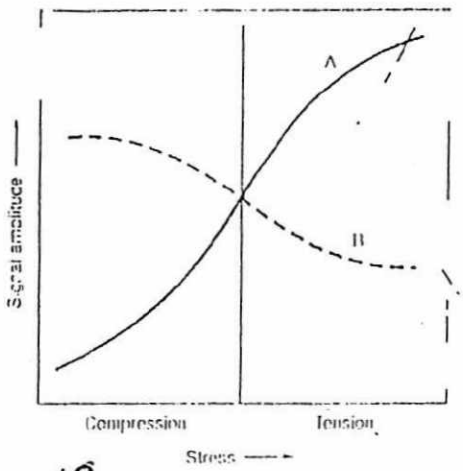

Fig. 10 Typical stress dependence of Barkhausen noise signal amplitude with the applied magnetic field parallel (curve A) and perpendicular (curve B) to the stress direction

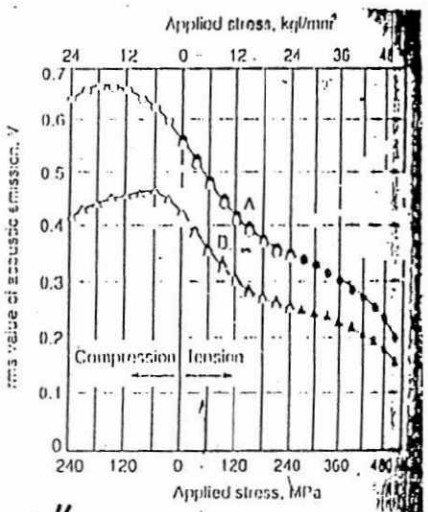

Fig. 11 Dependence of acoustic emission during magnetization of low-carbon steel on stress. Total gain 80 dB. Magnetic field strength (rms value) 13 000 A/m (160 Oe) for curve A; 6400 A/m (80 Oe) for curve B. Source: Ref 13

Table 1 A Compiled Summary of the Maximum Residual Stresses in Surface Heat Treated Steels[28]

Steel	*Heat Treatment*	*Residual Stress (Longitudinal) (N/mm^2)*
832M13 (type)	Carburized at 970°C to 1 mm case with 0.8% surface carbon	
	Direct-quenched	280
	Direct-quenched, −80°C subzero treatment	340
	Direct-quenched, −90°C subzero treatment, tempered	200
805A20	Carburized and quenched	240–340[a]
805A20	Carburized to 1.1–1.5 mm case	190–230
805A17	at 920°C, direct oil-quench, no temper	400
805A17	Carburized to 1.1–1.5 mm case at 920°C, direct oil-quench, tempered 150°C	150–200
897M39	Nitrided to case depth of about 0.5 mm	400–600
905M39		800–1000
Cold-rolled steel	Induction-hardened, untempered	1000
	Induction-hardened, tempered 200°C	650
	Induction-hardened, tempered 300°C	350
	Induction-hardened, tempered 400°C	170